Bioorganic & Medicinal Chemistry 18 (2010) 4067–4073

Contents lists available at ScienceDirect

Bioorganic & Medicinal Chemistry

journal homepage: www.elsevier.com/locate/bmc

Self-association of cyclic oligonucleotides through G:T:G:T minor groove tetrads

Júlia Viladoms [a,1], Núria Escaja [a], Enrique Pedroso [a,*], Carlos González [b,*]

[a] Departament de Química Orgànica and IBUB, Universitat de Barcelona, C/. Martí i Franquès 1-11, 08028 Barcelona, Spain
[b] Instituto de Química Física Rocasolano, CSIC, C/. Serrano 119, 28006 Madrid, Spain

ARTICLE INFO

Article history:
Received 23 November 2009
Revised 1 April 2010
Accepted 6 April 2010
Available online 13 April 2010

Keywords:
Unusual DNA structures
Cyclic oligonucleotides
Quadruplex
Tetrads
NMR spectroscopy

ABSTRACT

Minor groove aligned tetrads resulting from the association of Watson–Crick base pairs stabilize a distinct class of four-stranded DNA structures, different from G-quadruplexes or i-motifs. These tetrads can be formed by several arrangements of G–C or A–T base pairs. Here we prove that minor groove tetrads can be also formed by G–T mismatches. In this manuscript we describe the dimeric solution structures of two cyclic oligonucleotides stabilized by intermolecular G–T non-canonical base pairs. In the dimeric structure of d<pTCGTATGT>, these mismatches interact to each other giving rise to minor groove aligned G:T:G:T or mixed G:T:G:C tetrads. Interestingly, the stability conferred by mismatched G–T containing tetrads is similar to that of minor groove tetrads solely formed by G–C Watson–Crick base pairs.

1. Introduction

Although many of the non-canonical DNA structures were discovered decades ago, the importance of these structures in Chemistry and Biology has become more apparent in the last few years.[1] In particular, four-stranded structures have attracted extensive interest for their implication in biological processes, such as telomere maintenance or transcription regulation, or in supramolecular chemistry and nanotechnology.[2] The most studied four-stranded motif is the G-quadruplex, formed by two or more planar G-tetrads. On occasions, these quadruplexes may contain other kind of tetrads, such as those consisting of Watson–Crick base pairs[3–7] or mismatches.[8]

Minor groove aligned tetrads that result from the association of Watson–Crick base pairs form a singular class of four-stranded DNA structures, which differ from G-quadruplexes or i-motifs. These tetrads, which can be formed by different arrangements of G–C and A–T base pairs, have been observed in the crystal and solution structures of several oligonucleotides and as contacts between different duplexes in higher order crystalline DNA structures.[9,10] Until now, five different types of minor groove tetrads have been observed: A:T:A:T,[11,12] G:C:G:C direct,[11,13] G:C:G:C slipped,[14] C:G:G:C[15] and G:C:A:T.[16] Although they have been found in folded back linear oligonucleotides,[15] they are more easily studied in cyclic analogues, where the formation of competing duplex-like structures is impeded by chain cyclization.

Cyclic oligodeoxyribonucleotides have been used to study other non-canonical DNA structures, such as hairpins,[17,18] cruciforms[19] and guanine quadruplexes.[20] The availability of synthetic methods to obtain large amounts of cyclic oligoribo-[21,22] and oligodeoxyribonucleotides[23] has opened the possibility of using their interesting molecular recognition properties in a number of fields. Firstly, cyclic oligonucleotides can be used to target single-stranded DNA[24,25] and RNA[26] with higher affinity and selectivity than their linear counterparts. Secondly, dumbbells can acts as aptamers[27,28] and transcription factor decoys.[29,30] Finally, small cyclic ribodinucleotides, such as c-di-AMP[31] and c-di-GMP,[32] are important second messenger signaling molecules that regulate many processes in bacteria. The recognition of c-di-GMP by its cognate riboswitch has recently been described and the co-crystal structure determined.[33,34] Interestingly, c-di-GMP is recognized by the riboswitch using canonical and non-canonical base-pairing as well as intercalation.

The aim of this work is to investigate whether minor groove tetrads can be also formed by mismatched base pairs. Mismatches occur in genomic DNA as a consequence of natural processes such as recombination or replication. Among them, G–T is the most common mismatch, as it can also arise from cytosine methylation and deamination. The mismatched bases adopt a wobble structure, as originally proposed by Crick,[35] where guanine is shifted towards the minor groove while thymine is shifted towards the major groove, giving rise to two hydrogen bonds: H3T–O6G and H1G–O2T (Scheme 1A). G–T base pairs have been observed in crystals

* Corresponding authors. Tel.: +34 934034824; fax: +34 933397878 (E.P.); tel.: +34 915619400; fax: +34 915642431 (C.G.).
E-mail addresses: epedroso@ub.edu (E. Pedroso), cgonzalez@iqfr.csic.es (C. González).
[1] Present address: The Skaggs Institute for Chemical Biology, The Scripps Research Institute, 10550 North Torrey Pines Road, 92037 La Jolla, San Diego, CA.

0968-0896/$ - see front matter © 2010 Elsevier Ltd. All rights reserved.
doi:10.1016/j.bmc.2010.04.018

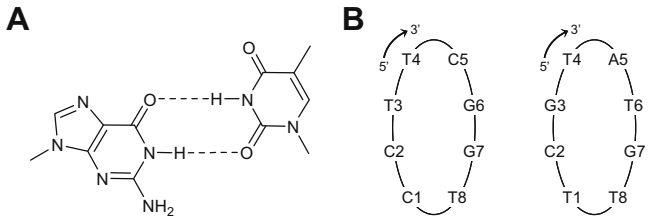

Scheme 1. (A) The wobble G–T pair. (B) Cyclic oligonucleotides prepared for this study: d<pCCTTCGGT> and d<pTCGTATGT>.

of A-, B- and Z-DNA with a minimal distortion of the global conformation and only small changes in the adjacent base pairs.[36] The base pair may be stabilized by additional hydrogen bond contacts through water molecules. This type of mismatch has also been observed in solution by NMR,[37–39] forming a wobble base pair with little deformation of the duplex structure.

To investigate the compatibility of G–T base pairs with minor groove tetrads, we have studied the structure and stability of the cyclic octamers d<pCCTTCGGT> and d<pTCGTATGT> (Scheme 1B).

2. Results and discussion

2.1. Complex formation and thermal denaturation

1D imino proton NMR spectra shown in Figure 1C clearly indicate that the two cyclic octamers adopt well defined structures. The imino signals observed between 13.0 and 14.0 ppm indicate the formation of G–C Watson–Crick base pairs, whereas the sharp signals between 11.0 and 12.5 ppm suggest the formation of G–T mismatches. The broader imino signals between 10.0 and 11.0 ppm correspond to the unpaired thymine imino protons. NMR melting experiments (Fig. 1C) indicate that the structure adopted by d<pCCTTCGGT> is not very stable. In contrast, imino signals of d<pTCGTATGT> can be observed above 45 °C, indicating that this structure is remarkably stable.

Melting transitions were also monitored by CD spectroscopy at different oligonucleotide concentrations, ranging from 65 to 500 μM. In all cases, the CD spectra at low temperature exhibit a large positive band around 260–270 nm and a negative band around 245 nm. Both bands disappear as the temperature increases (Fig 1A). At oligonucleotide concentrations similar to those employed in the NMR experiments, melting temperatures of the d<pCCTTCGGT> and d<pTCGTATGT> are 34 °C and 55 °C, respectively. The formation free energies (25 °C) resulting from the analysis of the melting curves are −24 kJ/mol for d<pCCTTCGGT> and −40 kJ/mol for d<pTCGTATGT> (Table 1).

NMR spectra of both oligonucleotides exhibit a strong dependence on oligonucleotide concentration (Fig. 1D). Also, melting transitions are concentration dependent (Fig. 1B). These data indicate that the structures are not monomeric. The similarity with the NMR spectra of other cyclic oligonucleotides of the same family, including the chemical shifts of some key signals as well as a number of characteristic NOE cross-peaks,[14] led us to conclude that both molecules adopt dimeric structures in solution. Note that the conformational constraint induced by the cyclization impedes the formation of higher order structures with Watson–Crick base pairs.[15]

2.2. NMR assignment

The assignment of most resonances of the NMR spectra of d<pCCTTCGGT> and d<pTCGTATGT> could be carried out following standard techniques (see Tables SI1 and SI2 in Supplementary data). With the exception of some split signals in the spectra of d<pTCGTATGT> that will be discussed below, the number of resonances in the spectra of both molecules corresponds to eight nucleotides, indicating that the dimers are symmetric. Residues 1–8 are magnetically equivalent to residues 9–16 (see Scheme 1B and Fig. 4 for numbering). In the following discussion the equivalent residues are indicated in brackets. The assignment of non-exchangeable resonances was facilitated by the strong similarities with previously studied dimeric structures stabilized by minor groove tetrads. The exchangeable proton spectra are particularly informative. Intermolecular G–C Watson–Crick base pairs are assessed by the NOE contacts H5C→NH2C H1G→NH2G. In both cases, the presence of G–T mismatches is confirmed by the characteristic chemical shift of the H-bonded imino protons H3T and H1G, which resonate between 10 and 12.5 ppm, and the cross-peaks between them. H3T and H1G could be distinguished by the NOE cross-peaks of H1G with their own amino protons (Fig. 2).

2.3. Structural features derived from NMR data

In the case of d<pCCTTCGGT> imino–imino cross-peak arises from H3T3(11) and H1G14(6) (Fig. SI1). The two amino protons of G6(14) are degenerate and resonate at 5.8 ppm, indicating that they are not involved in hydrogen bonds. However, these amino protons exhibit NOE contacts with the imino and amino protons of the neighboring G7(15). Watson–Crick base pairs occur between G7(15) and C10(2). Other additional contacts, including H1′ of G7(15) with H21/H22 of G15(7), can only be assigned as intermolecular and they are consistent with the formation of a slipped G7:C10:G15:C2 minor groove tetrad.[14]

Interestingly, the NMR spectra of d<pTCGTATGT> are somewhat more complex. Although many features of the spectra are similar to those of d<pCCTTCGGT>, some resonances are split, in particular most of the exchangeable protons, and a few of the non-exchangeable ones (Fig. 2 and Table SI2). The NMR spectra are consistent with an equilibrium between two conformers in slow exchange on the NMR time scale. Since the splitting only affects some resonances, and it is observed at different oligonucleotide concentrations (Fig. 1D), we conclude that both conformers are symmetric dimers of very similar structure. The distinct structural features between them can be assessed mainly on the basis of exchangeable proton contacts. In both cases, the characteristic pattern of NOEs for G–C and G–T base pairs is observed (Fig. 2). The additional contacts: H1′G3(G11)–H1/H21/H22G11(G3) and H1′G7(G15)–H1/H21/H22G15(G7), for the first species, and H1′G3′(G11′)–H22G15′(G7′) and H1′G7′(G15′)–H22G11′(G3′) for the second one (denoted with primes) clearly indicate the formation of two slipped tetrads: G7:C10:G15:C12 and T6:G11:G3:T14 for the first species, and G7:T14:G11:C2 and T6:G15:G3:C10 for the second one, as will be discussed below. The signals of both species show similar intensities, indicating that their populations are approximately equal. Coalescence between the signals of the two forms is not achieved before the melting, showing that the equilibrium between both species is slow on the NMR time scale over the entire temperatures range (Fig. 1C). Different experimental conditions, like moderate changes in the pH or ionic strength (data not shown), do not appear to alter the relative populations between these two conformers.

Many spectral features are characteristic of dimeric structures stabilized by minor groove tetrads. All intra-nucleotide H1′-base NOEs are medium or weak, indicating that the glycosidic angle in all the nucleotides is in an *anti* conformation. Also, sequential NOE sugar-base cross-peaks are observed for residues 2(10)–3(11)–4(12) and 6(14)–7(15)–8(16), but these sequential NOEs are not observed for the residues in the second position of the loops, 1(9) and 5(13). A number of NOE contacts between the methyl groups of T4(12) and T8(16) and the adjacent base pairs

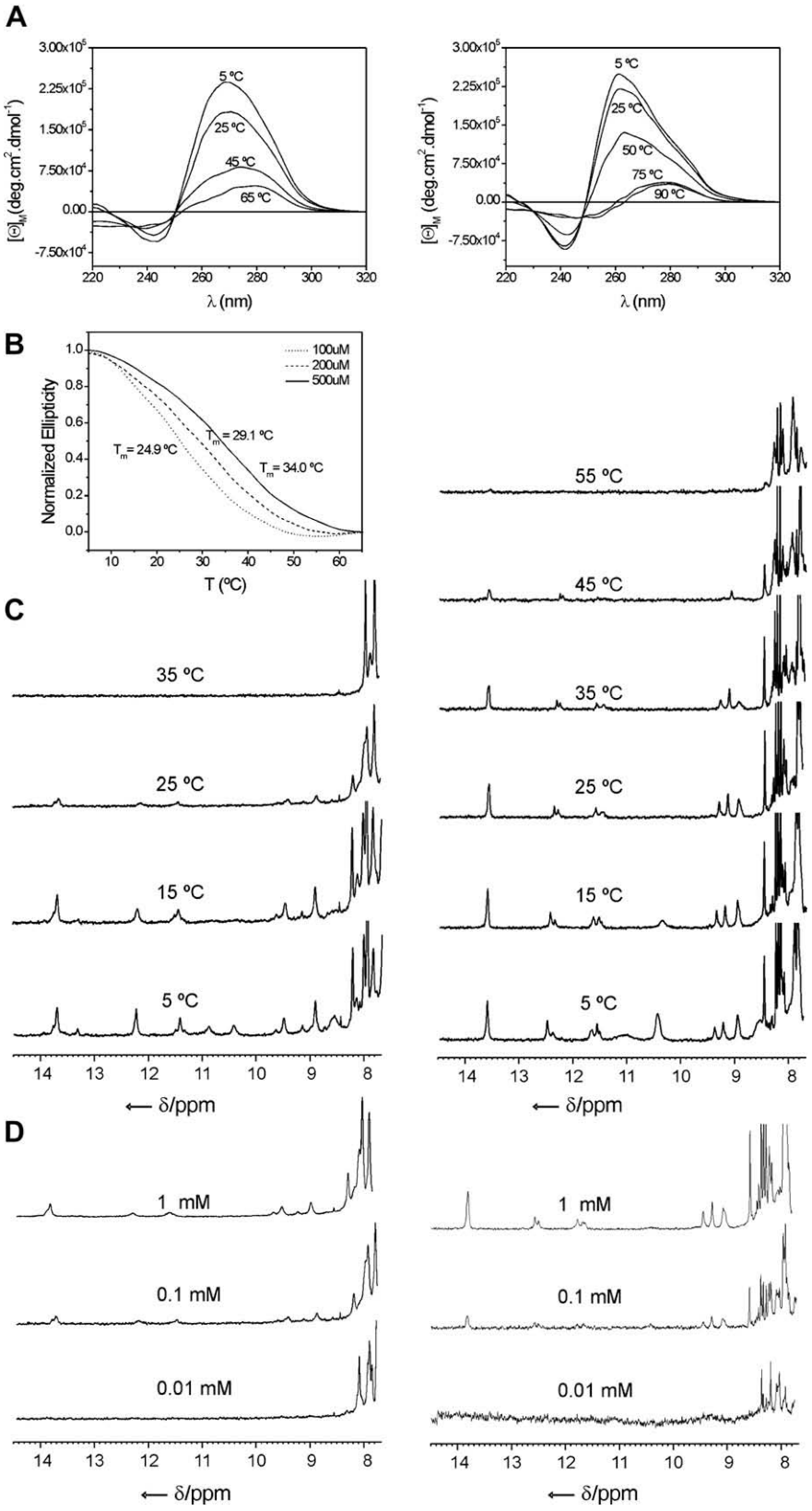

Figure 1. (A) CD spectra of d<pCCTTCGGT> (500 μM) (left) and d<pTCGTATGT> (330 μM) (right) at different temperatures. (B) Melting curves of d<pCCTTCGGT> at different oligonucleotide concentrations. (C) 1D NMR spectra of d<pCCTTCGGT> (2 mM) (left) and d<pTCGTATGT> (1 mM) (right) at different temperatures. (D) 1D NMR spectra of d<pCCTTCGGT> (left) and d<pTCGTATGT> (right) at different oligonucleotide concentration (T = 5 °C). Buffer conditions for all experiments: 25 mM sodium phosphate, 100 mM NaCl, 50 mM $MgCl_2$, pH 7.

indicate that these thymines are stacked on top of the G–C or G–T base pairs. In the case of T4 of d<pCCTTCGGT>, in which this stacking occurs on top of a guanine residue, anomalously low chemical shifts for H4′, H5′ and H5″ are observed.

Table 1
Thermodynamic parameters for the formation of the dimeric species of d<pCCTTCGGT> (500 μM oligonucleotide concentration) and d<pTCGTATGT> (330 μM oligonucleotide concentration)

Parameters	d<pCCTTCGGT>	d<pTCGTATGT>
ΔH° (kJ/mol)	−146	−214
ΔS° (J/mol K)	−412	−585
ΔG°_{298} (kJ/mol)	−24	−40

Buffer conditions: 25 mM sodium phosphate pH 7, 100 mM NaCl, 50 mM $MgCl_2$.

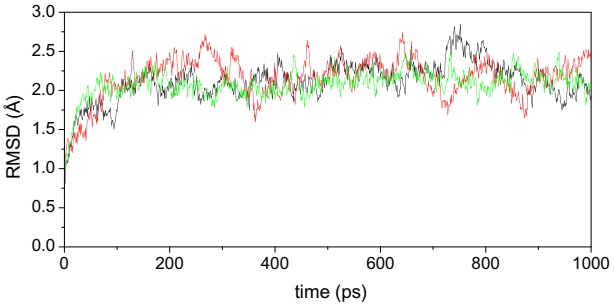

Figure 3. RMSD along the trajectories of d<pCCTTCGGT> (red), the first species of d<pTCGTATGT> (black) and the second species of d<pTCGTATGT> (green). The RMSDs are calculated with respect to the initial structure for all heavy atoms except those of the second residues of the loops which exhibit an increased mobility.

2.4. Structure calculation

The presence of several species in slow exchange, where some of their signals are degenerated, impedes the extraction of accurate distance constraints from a number of NOE cross-peaks. However, the NMR data is sufficient to build reliable models of these structures (see Table SI3 for a list of unambiguously assigned NOE cross-peaks). Models of the dimeric structures of d<pCCTTCGGT> and the two species of d<pTCGTATGT> were constructed on the basis of the average dimeric structure of d<pCCGTCCGT>.[14] After performing the appropriate mutations for each molecule with the program SYBYL, the three models were submitted to 1 ns runs of state-of-the-art molecular dynamics calculations with the AMBER package (see Section 4 for details). No distance constraints or hydrogen bond constraints were included in these calculation. In spite of that, the three trajectories are stable (see Fig. 3) and converge to structures that are consistent with the experimental data. Thus, in addition to the above-mentioned NOEs, corresponding to exchangeable protons involved in base pairs, the calculated structures are consistent with the key observed NOEs shown in Table SI3.

Resulting models are shown in Figure 4, and present many features in common with other members of this family of structures. In all cases, the oligonucleotides adopt a symmetric dimeric structure in which the two circles run antiparallel to each other. The structures are stabilized by two stacks of intermolecular G–C and G–T base pairs that exhibit a mutual inclination of around 30–40°. The thymines located in the first position of the loops form two caps at both ends of the stacks. Residues in the second position of the loops are solvent exposed.

2.5. The structure of d<pCCTTCGGT>

The dimer formed by d<pCCTTCGGT> is stabilized by one slipped minor groove G:C:G:C tetrad and two additional wobble G–T base pairs. Although the spatial arrangement of these G–T base pairs resembles that of a direct G:C:G:C minor grove tetrad found, for example, in the dimeric structure of d<pTGCTCGCT>[11] (Fig. 5), in this case there are no hydrogen bonds between the guanines of two G–T base pairs. The lack of additional stabilizing interaction between the two mismatches is reflected in the low thermal stability of this dimer, which is 16 kJ/mol less stable than the ones formed by d<pTCGTATGT> (Table 1).

In light of the structure, none of the two G6(14) amino protons are involved in hydrogen bonds. These amino protons are not exposed to the solvent, but buried in the center of the structure. This

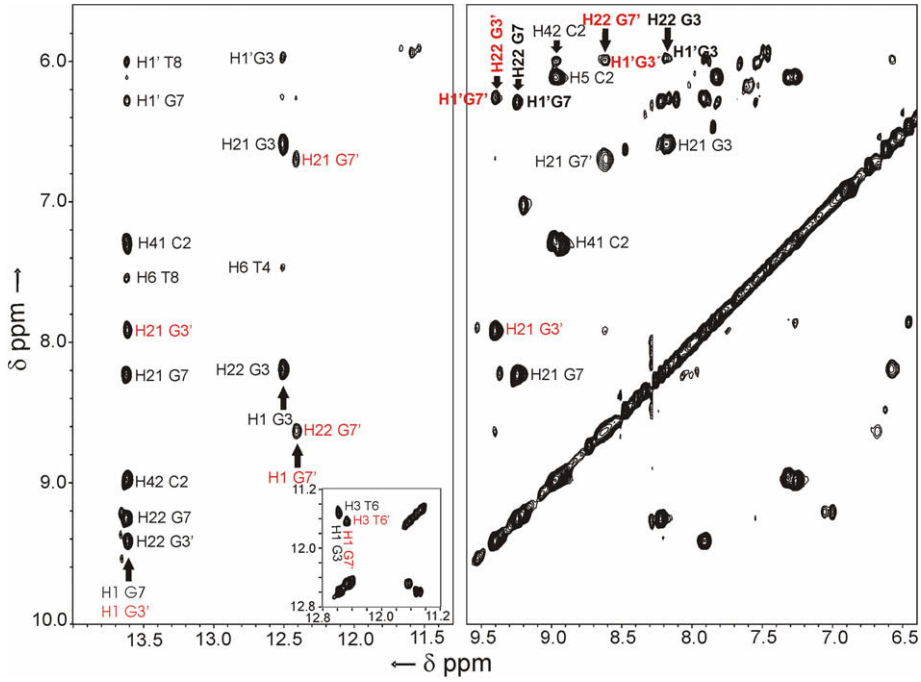

Figure 2. Exchangeable proton region of NOESY spectrum (150 ms) of d<pTCGTATGT> at 2 mM oligonucleotide concentration showing some key contacts in bold. Labels of signals corresponding to the second conformer are shown in red and denoted with primes.

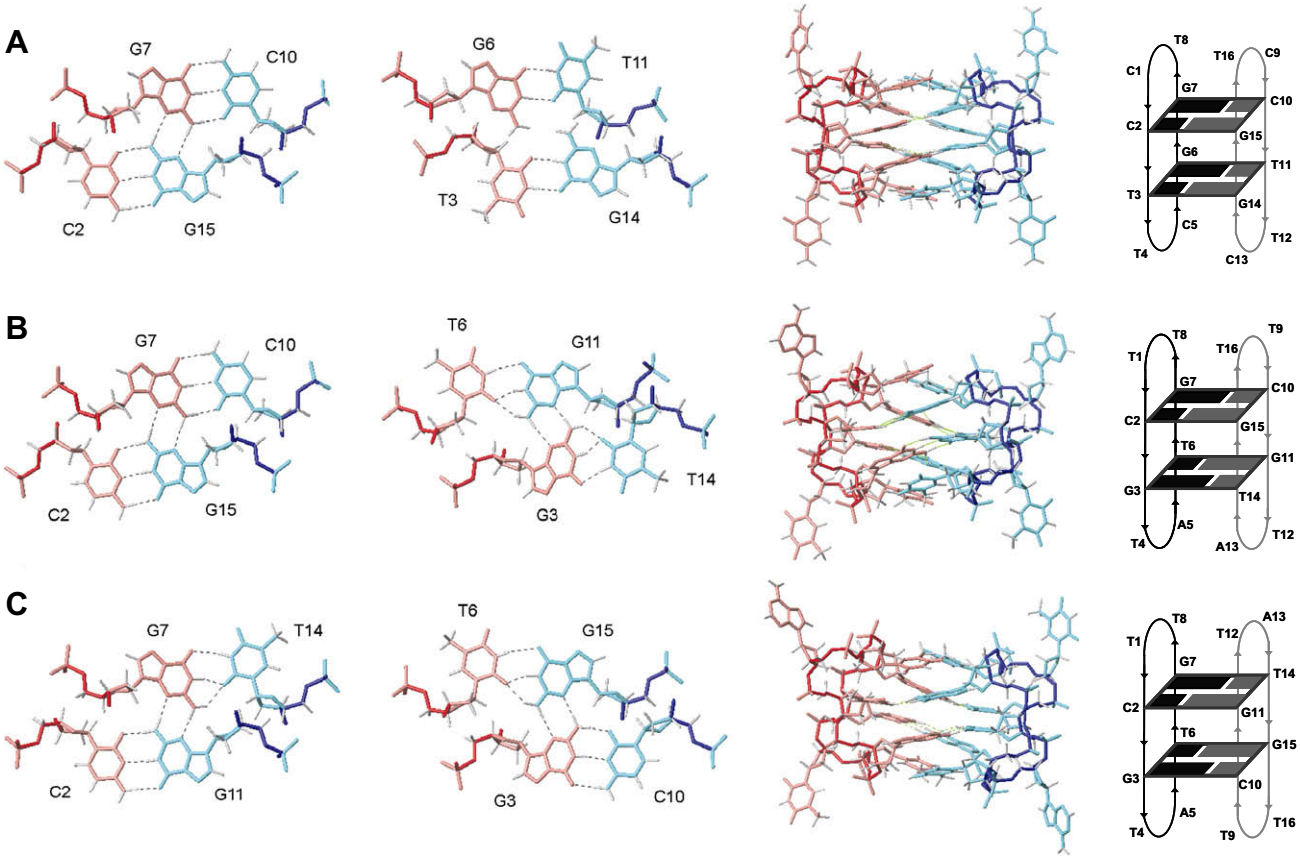

Figure 4. Structures resulting from the molecular dynamics calculations: (A) d<pCCTTCGGT>, (B) first species of d<pTCGTATGT>, and (C) second species of d<pTCGTATGT>. (Left) Details of the two tetrads that stabilize each dimer. (Middle) Average structures. (Right) Schemes of the dimers. Red and blue indicate different molecules. The sugar–phosphate backbone is indicated in darker colors.

is consisting with their chemical shifts (5.8 ppm), and the number of NOEs observed with the amino protons of the neighboring G7(15).

2.6. The structure of d<pTCGTATGT>

On the other hand, the dimers formed by d<pTCGTATGT> are stabilized by two slipped minor groove tetrads. The fact that a single transition is observed in the CD denaturation curves, and that proton NMR signals from the two species exhibit similar intensities, clearly show that both dimers have a very similar formation free energy. These two conformers correspond with two possible arrangements of the two circles. In one of them the slipped tetrads are formed by G7:C10:G15:C2 and G3:T14:G11:T6. In the other conformer, the two circles are rotated 180° with respect to each other, and form two slipped G:C:G:T tetrads (G3:C10:G15:T6 and G11:C2:G7:T14). In both conformers the number of G–T and G–C base pairs is the same, and the interaction between the base pairs in all the tetrads occurs through two hydrogen bonds H2G–N3G between the two guanine residues. Since the chemical environment of all the protons is almost identical, we must conclude that both conformers adopt structures that, locally, are very similar and contain equivalent stabilizing interactions. This explains the degeneration of the chemical shifts of most protons in both species and the energetic equivalence between the two conformers.

In the calculated structure of d<pTCGTATGT>, the G–T mismatches are not the standard wobble G–T base pairs, but are slightly distorted and exhibit bifurcated hydrogen bonds between the guanine amino proton and H1 with thymine O2. The two guanine amino protons of d<pTCGTATGT> involved in G–T base pairs resonate between 6.6 and 8.7 ppm, whereas unpaired amino protons usually present lower chemical shifts. The low field shift of the two guanine amino protons is an experimental confirmation of the presence of bifurcated hydrogen bonds. Such pattern of hydrogen bonds is not common in G–T base pairs, but it has been observed before in a DNA duplex containing tandem G–T mismatches.[40]

It is interesting to compare the formation free energy of d<pTCGTATGT> with other structures of the same family. Although the buffer conditions are not identical, the formation free energy of d<pTCGTATGT> is in the same range as that of dimeric structures stabilized by G:C:G:C or C:G:G:C minor groove tetrads.[15] Since G:C:G:C and C:G:G:C minor groove tetrads have been found in quadruplex structures formed linear oligonucleotides,[13,15] this result suggests that mismatched G–T minor groove tetrads may confer enough stability to enable the formation of similar structures in linear oligonucleotides.

2.7. Minor versus major groove G:T:G:T tetrads

G:T:G:T tetrads have been previously observed in the context of G-quadruplexes[8] and i-motif structures.[41] Balasubramanian et al. observed G:T:G:T tetrads in interlocked parallel quadruplexes formed by the sequence d(GGGT).[8] These tetrads consist of two G–T mismatches, with H3T–O6G and H1G–O4T hydrogen bonds, that interact through their major groove sides forming two additional hydrogen bonds between one of the amino protons of G and O4T (Fig. 5B). On the other hand, a G:T:G:T tetrad that resembles the minor groove slipped G:T:G:T tetrad found in this work

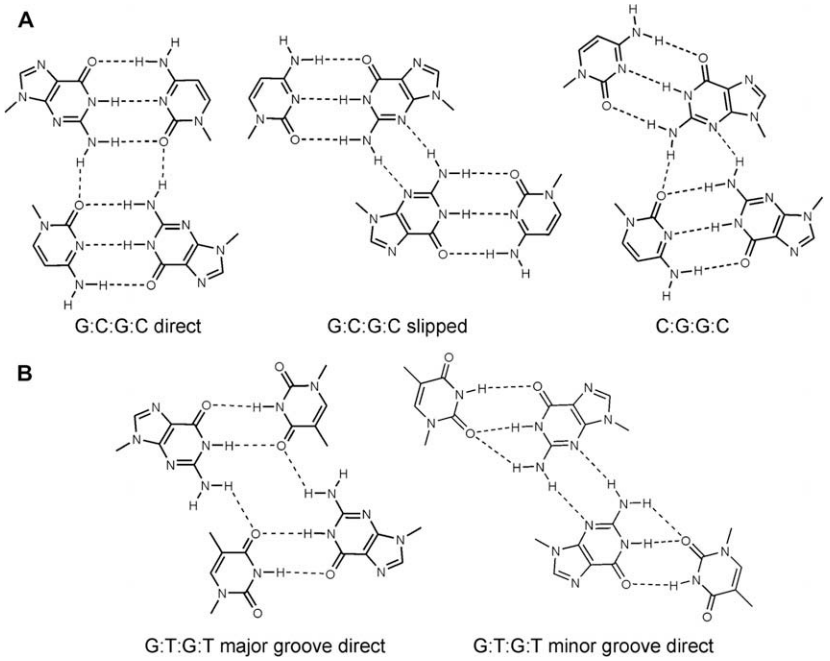

Figure 5. (A) Minor groove tetrads stabilized by GC base pairs. (B) Comparison of GT base pairs in major (left) and minor (right) groove tetrads.

has been observed in the solution structures of two oligonucleotides related to the centromeric pyrimidine strand.[41] At low pH, the oligonucleotides d(TCCCGTTTCCA) and d(CCCGTTCC) form hairpins that dimerize in solution through the formation of C–C^+ intercalated base pairs. The GTTT loops form two wobble G–T base pairs, with H3T–O6G and H1G–O2T hydrogen bonds. The guanines of these G–T base pairs interact to each other through two hydrogen bonds H2G–N3G. Although the resulting minor groove tetrad observed in this structure is similar to the slipped G:T:G:T tetrad found in the structure of d<pTCGTATGT>, no bifurcated hydrogen bonds are observed in the former. The G:T:G:T tetrad observed in the loop of the i-motif hairpins studied by Gallego et al.[41] is formed by canonical wobble G–T mismatches. Interestingly, both G:T:G:T tetrads are not planar but there is a mutual inclination between the two G–T mismatches. In contrast, the major groove G:T:G:T tetrad observed in interlocked G-quadruplexes is presumably planar.[8]

3. Conclusions

In summary, we have shown that, like canonical Watson–Crick base pairs, G–T mismatches can be involved in minor groove tetrads. These tetrads can result from the association of two G–T base pairs or the combination of a G–C and a G–T base pair. In both cases the arrangement of the two base pairs is very similar to the slipped minor groove G:C:G:C tetrad described previously. Overall, the dimeric structures formed by slipped minor groove G:C:G:T or G:T:G:T tetrads are very similar to other structures stabilized by minor groove tetrads, and exhibit a similar stability to those formed by G:C:G:C or C:G:G:C tetrads.

4. Experimental section

The cyclic octamers were synthesized as reported by Alazzouzi et al.[23] and purified by HPLC or PAGE. Cyclic oligonucleotides were characterized by enzymatic digestion, that gave the right proportion of nucleosides, and MALDI-TOF mass spectrometry (d<pCCTTCGGT>: *M* calculated = 2437.38 amu, *m*/*z* = 2437.37 amu; d<pTCGTATGT>: *M* calculated = 2476.39 amu, *m*/*z* = 2473.38 amu).

Samples for NMR were suspended (as Na^+ salts) in either D_2O or 9:1 H_2O/D_2O (100 mM NaCl, 10 mM $MgCl_2$, sodium phosphate buffer, pH 7).

4.1. Circular dichroism

Circular dichroism spectra were collected on a Jasco J-810 spectropolarimeter fitted with a thermostated cell holder. For melting experiments, the samples were initially heated at 90 °C for 5 min, and slowly cooled to room temperature and stored at 4 °C until use. CD melting experiments were recorded at 0.5 °C/min at the maximum wavelength. At this temperature change rate no difference is observed between the melting and annealing profiles. CD spectra were recorded at concentrations of the complexes ranging from 300 to 500 μM. The spectra were normalized to facilitate comparisons. Thermodynamic parameters were calculated from single melting curves, by representing $\ln K$ versus $1/T$ (for $0.15 < x < 0.85$).[42]

$$x(t) = \frac{\mathrm{CD}(t) - \mathrm{CDdenat}(t)}{\mathrm{CDstruc}(t) - \mathrm{CDdenat}(t)} \qquad K_a = \frac{x}{2c_0(1-x)^2}$$

$$\ln K = -\frac{\Delta H^0}{R}\cdot\frac{1}{T} + \frac{\Delta S^0}{R}$$

4.2. NMR spectroscopy

All NMR spectra were acquired in Bruker spectrometers operating at 600 MHz or 800 MHz, equipped with cryoprobes and processed with the TOPSPIN software. In the experiments in D_2O, presaturation was used to suppress the residual H_2O signal. A jump-and-return pulse sequence[43] was employed to observe the rapidly exchanging protons in 1D H_2O experiments. NOESY spectra in D_2O were acquired with mixing times of 100 and 250 ms. TOCSY spectra were recorded with the standard MLEV-17 spin-lock sequence and a mixing time of 80 ms. In 2D experiments in H_2O, water suppression were achieved by including a WATERGATE[44] module in the pulse sequence prior to acquisition. NOESY spectra in H_2O were acquired with a mixing time of

150 ms. The spectral analysis program SPARKY[45] was used for semi-automatic assignment of the NOESY cross-peaks.

4.3. Model building and molecular dynamics calculations

Models of the dimeric structures of d<pTCGTATGT> and d<pCCTTCGGT> were built from the dimeric structure of d<pCCGTCCGT>, previously calculated in our group.[14] The appropriate residues were mutated with the program SYBYL, preserving the geometry of the original model, and then minimized in vacuo. The structures were immersed in a water box of around 3000 water molecules. The whole system was then submitted to the standard equilibration protocol used in our group[46] and to a long run of 1 ns of unconstrained molecular dynamics calculation with the molecular dynamics package AMBER.[47] The AMBER-98 force-field[48] was used to describe the DNA, and the TIP3P model was used to simulate water molecules.[49] The Particle Mesh Ewald method was used to evaluate long-range electrostatic interactions.[50] The last 25 ps of each trajectory were averaged and then minimized. The analysis of the final structures as well as the molecular dynamics trajectories was carried out with the program MOLMOL.[51]

Acknowledgements

We gratefully acknowledge Dr. D.V. Laurents for revision of the manuscript and his useful comments. This work was supported by the Spanish MICINN (Grants CTQ2007-68014-C02-01/02) and Generalitat de Catalunya (2005SGR693 and Xarxa de Referència en Biotecnologia).

Supplementary data

Supplementary data associated with this article can be found, in the online version, at doi:10.1016/j.bmc.2010.04.018.

References and notes

1. Belmont, P.; Constant, J. F.; Demeunynck, M. *Chem. Soc. Rev.* **2001**, *30*, 70; Bacolla, A.; Wells, R. D. *J. Biol. Chem.* **2004**, *279*, 47411; Neidle, S.; Balasubramanian, S. *Quadruplex Nucleic Acids*; RSC Publishing: Cambridge, UK, 2006; Mirkin, S. M. *Front. Biosci.* **2008**, *13*, 1064.
2. Davis, J. T. *Angew. Chem., Int. Ed.* **2004**, *43*, 668.
3. Webba da Silva, M. *Biochemistry* **2003**, *42*, 14356.
4. Webba da Silva, M. *Biochemistry* **2005**, *44*, 3754.
5. Kettani, A.; Bouaziz, S.; Gorin, A.; Zhao, H.; Jones, R. A.; Patel, D. J. *J. Mol. Biol.* **1998**, *282*, 619.
6. Kettani, A.; Kumar, R. A.; Patel, D. J. *J. Mol. Biol.* **1995**, *254*, 638.
7. Zhang, N.; Gorin, A.; Majumdar, A.; Kettani, A.; Chernichenko, N.; Skripkin, E.; Patel, D. J. *J. Mol. Biol.* **2001**, *312*, 1073.
8. Krishnan-Ghosh, Y.; Liu, D.; Balasubramanian, S. *J. Am. Chem. Soc.* **2004**, *126*, 11009.
9. Tereshko, V.; Subirana, J. A. *Acta Crystallogr., D Biol. Crystallogr.* **1999**, *55*, 810.
10. Wahl, M. C.; Sundaralingam, M. In *Oxford Handbook of Nucleic Acid Structures*; Neidle, S., Ed.; Oxford University Press: New York, 1999; pp 389–453.
11. Escaja, N.; Pedroso, E.; Rico, M.; González, C. *J. Am. Chem. Soc.* **2000**, *122*, 12732.
12. Salisbury, S. A.; Wilson, S. E.; Powell, H. R.; Kennard, O.; Lubini, P.; Sheldrick, G. M.; Escaja, N.; Alazzouzi, E.; Grandas, A.; Pedroso, E. *Proc. Natl. Acad. Sci. U.S.A.* **1997**, *94*, 5515.
13. Leonard, G. A.; Zhang, S.; Peterson, M. R.; Harrop, S. J.; Helliwell, J. R.; Cruse, W. B.; d'Estaintot, B. L.; Kennard, O.; Brown, T.; Hunter, W. N. *Structure* **1995**, *3*, 335.
14. Escaja, N.; Gomez-Pinto, I.; Pedroso, E.; González, C. *J. Am. Chem. Soc.* **2007**, *129*, 2004.
15. Viladoms, J.; Escaja, N.; Frieden, M.; Gómez-Pinto, I.; Pedroso, E.; Gonzalez, C. *Nucleic Acids Res.* **2009**, *37*, 3264.
16. Escaja, N.; Gelpi, J. L.; Orozco, M.; Rico, M.; Pedroso, E.; González, C. *J. Am. Chem. Soc.* **2003**, *125*, 5654.
17. Ippel, J. H.; Lanzotti, V.; Galeone, A.; Mayol, L.; Van den Boogaart, J. E.; Pikkemaat, J. A.; Altona, C. *J. Biomol. NMR* **1995**, *6*, 403.
18. Escaja, N.; Gomez-Pinto, I.; Rico, M.; Pedroso, E.; Gonzalez, C. *ChemBiochem* **2003**, *4*, 623.
19. Lin, C.-T.; Lyu, Y. L.; Liu, L. F. *Nucleic Acids Res.* **1997**, *25*, 3009.
20. Casals, J.; Viladoms, J.; Pedroso, E.; Gonzalez, C. *J. Nucleic Acids*, **2010**, *2010*. doi:10.4061/2010/468017.
21. Micura, R. *Chem. Eur. J.* **1999**, *5*, 2077.
22. Frieden, M.; Grandas, A.; Pedroso, E. *Chem. Commun.* **1999**, *16*, 1593.
23. Alazzouzi, E.; Escaja, N.; Grandas, A.; Pedroso, E. *Angew. Chem., Int. Ed.* **1997**, *36*, 1506.
24. Escaja, N.; Gómez-Pinto, I.; Viladoms, J.; Rico, M.; Pedroso, E.; González, C. *Chem. Eur. J.* **2006**, *12*, 4035.
25. Prakash, G.; Kool, E. T. *J. Am. Chem. Soc.* **1992**, *114*, 3523.
26. Prakash, G.; Kool, E. T. *J. Chem. Soc., Chem. Commun.* **1991**, *1161*.
27. Hannoush, R. N.; Carreiro, S.; Min, K. L.; Damha, M. J. *ChemBioChem* **2004**, *5*, 527.
28. Di Giusto, D. A.; King, G. C. *J. Biol. Chem.* **2004**, *275*, 46483.
29. Lim, C. S.; Jabrane-Ferrat, N.; Fontes, J. D.; Okamoto, H.; Garovoy, M. R.; Peterlin, B. M.; Hunt, C. A. *Nucleic Acids Res.* **1997**, *25*, 575.
30. Hosoya, T.; Takeuchia, H.; Kanesaka, Y.; Yamakawa, Y.; Miyano-Kurosaki, N.; Takaia, K.; Yamamoto, N.; Takakua, H. *FEBS Lett.* **1999**, *461*, 136.
31. Römling, G. C. *Sci. Signal.* **2008**, *1*, pe39.
32. Hengge, R. *Nat. Rev. Microbiol.* **2009**, *7*, 263.
33. Kulshina, N.; Baird, N. J.; Ferré-D'Amaré, A. R. *Nat. Struct. Mol. Biol.* **2009**, *16*, 1212.
34. Smith, K. D.; Lipchock, S. V.; Ames, T. D.; Wang, J.; Breaker, R. R.; Strobel, S. A. *Nat. Struct. Mol. Biol.* **2009**, *16*, 1218.
35. Crick, F. H. *J. Mol. Biol.* **1966**, *19*, 548.
36. Kennard, O. *J. Biomol. Struct. Dyn.* **1985**, *3*, 205.
37. Isaacs, R. J.; Rayens, W. S.; Spielmann, H. P. *J. Mol. Biol.* **2002**, *319*, 191.
38. Hare, D.; Shapiro, L.; Patel, D. J. *Biochemistry* **1986**, *25*, 7445.
39. Allawi, H. T.; SantaLucia, J., Jr. *Nucleic Acids Res.* **1998**, *26*, 4925.
40. Alvarez-Salgado, F.; Desvaux, H.; Boulard, Y. *Magn. Reson. Chem.* **2006**, *44*, 1081.
41. Gallego, J.; Chou, S. H.; Reid, B. R. *J. Mol. Biol.* **1997**, *273*, 840.
42. Petersheim, M.; Turner, D. H. *Biochemistry* **1983**, *22*, 256.
43. Plateau, P.; Güeron, M. *J. Am. Chem. Soc.* **1982**, *104*, 7310.
44. Piotto, M.; Saudek, V.; Sklenar, V. *J. Biomol. NMR* **1992**, *2*, 661.
45. Goddard, D. T.; Kneller, G. *SPARKY 3*, University of California, San Francisco.
46. Soliva, R.; Monaco, V.; Gómez-Pinto, I.; Meeuwenoord, N. J.; Marel, G. A.; Boom, J. H.; González, C.; Orozco, M. *Nucleic Acids Res.* **2001**, *29*, 2973.
47. Case, D.A.; Pearlman, D. A.; Caldwell, J. W.; Cheatham, T. E., III, Wang, J.; Ross, W. S.; Simmerling, C. L.; Darden, T. A.; Merz, K. M.; Stanton, R. V.; Cheng, A. L.; Vincent, J. J.; Crowley, M.; Tsui, V.; Gohlke, H.; Radmer, R. J.; Duan, Y.; Pitera, J.; Massova, I.; Seibel, G. L.; Singh, U. C.; Weiner, P. K.; Kollman P. A. *AMBER 7*, University of California, San Francisco, 2002.
48. Cornell, W. D.; Cieplak, P.; Bayly, C. I.; Gould, I. R.; Merz, K.; Ferguson, D. M.; Spellmeyer, D. C.; Fox, T.; Caldwell, J. W.; Kollman, P. A. *J. Am. Chem. Soc.* **1995**, *117*, 5179.
49. Jorgensen, W. L.; Chandrasekhar, J.; Madura, J. D.; Impey, R. W.; Klein, M. L. *J. Chem. Phys.* **1983**, *79*, 926.
50. Darden, T. E.; York, D.; Pedersen, L. *J. Chem. Phys.* **1993**, *98*, 10089.
51. Koradi, R.; Billeter, M.; Wüthrich, K. *J. Mol. Graphics* **1996**, *14*, 29.